WELDING RESEARCH

SUPPLEMENT TO THE *WELDING JOURNAL*, JULY 1987

Sponsored by the American Welding Society and the Welding Research Council

All papers published in the *Welding Journal's* Welding Research Supplement undergo Peer Review before publication for: 1) originality of the contribution; 2) technical value to the welding community; 3) prior publication of the material being reviewed; 4) proper credit to others working in the same area; and 5) justification of the conclusions, based on the work performed.

The names of the more than 170 individuals serving on the AWS Peer Review Panel are published periodically. All are experts in specific technical areas, and all are volunteers in the program.

Intermetallic Formation in Soldered Copper-Based Alloys at 150° to 250°C

The base metal nickel content and the solder tin content greatly influence the rate of intermetallic formation

BY E. K. OHRINER

ABSTRACT. The formation of intermetallic compounds on a number of copper-base alloys soldered with a variety of tin-containing solders has been studied for the temperature range 150° to 250°C (302° to 482°F) for exposure times of up to 4000 h. Pure copper and the alloy Cu-5Sn-0.2P form a layer of the intermetallic Cu_3Sn adjacent to the base metal and a second layer of Cu_6Sn_5 adjacent to the solder. The copper-nickel-tin alloys Cu-6Ni-4Sn, Cu-9Ni-6Sn, Cu-9Ni-2Sn, Cu-15Ni-8Sn, Cu-21Ni-5Sn, and Cu-23Ni-8Sn-3Co form the $(Cu,Ni)_6Sn_5$ intermetallic compound only. The thickness of the intermetallic layers is proportional to the square root of the exposure time for all alloy-solder combinations. When soldered with 95Sn-5Ag, 95Sn-5Sb, or 60Sn-40Pb solders, the rate of intermetallic formation is dependent on the nickel content of the alloy and exhibits a peak in the range of 6 to 9% nickel. The details of the compositional dependence vary with solder composition and exposure temperature. The ratio of parabolic rate constants (intermetallic thickness/square root time) of alloys of different nickel contents can be as large as 35. The rates of intermetallic formation with 10Sn-90Pb solder are lower than those for high-tin content solders, and at exposure temperatures of 225°C (437°F) and below, are much less sensitive to base metal composition. The results have important implications in the selection of solders used in elevated-temperature service.

KEY WORDS

Solder
Copper-Base Alloys
Cu-Ni-Sn Alloys
Intermetallic Compound
Cu_3Sn
Cu_6Sn_5
Beryllium-copper
Cu-15Ni-8Sn
Cu-5Sn-0.2P
High-Temp. Solder

E. K. OHRINER is a Research Metallurgist with Pfizer, Inc., Wallingford, Conn.

Introduction

Soldering of copper and copper-base alloys is generally performed using tin-containing solders. It is well known that tin from the solder will react with copper and copper-base alloys to produce intermetallic compounds at the interface with the solder. The reaction may occur during contact with molten solders or as a solid-state reaction. The formation of intermetallic layers has been studied for copper in molten tin (Ref. 1), and copper and copper alloys in molten tin-containing solders (Refs. 2, 3). Intermetallic formation between copper in contact with solid tin and tin-containing solders has been studied extensively (Refs. 4–7). Intermetallic formation has also been studied in connection with its effects on the solderability of plated copper, exposed to elevated temperature or stored for extended times at room temperature (Refs. 8–10), and on the mechanical properties of soldered joints exposed to elevated temperature (Refs. 11–15). These studies have been limited to pure copper or in a few instances to Cu-30Zn. The purpose of this study is to

RESEARCH/DEVELOPMENT/RESEARCH/DEVELOPMENT/RESEARCH/DEVELOPMENT/RESEARCH/DEVELOPMENT/RESEARCH/DEVELOPMENT

Table 1—Composition and Condition of Base Metals

Alloy Composition (wt-%)	UNS No.	Processing	Condition or Temper[a]
Copper (99.99%)		cast and wrought	20% cold rolled
Cu-5Sn-0.2P	C51000	cast and wrought	H04
Cu-1.9Be-0.4Co	C17200	cast and wrought	TM04
Cu-6Ni-4Sn	–	laboratory wrought P/M	25% cold rolled
Cu-9Ni-2Sn	C72500	cast and wrought	H04
Cu-9Ni-6Sn	C72700	cast and wrought	TM02
Cu-9Ni-6Sn	C72700	laboratory wrought P/M	25% cold rolled
Cu-15Ni-8Sn	C72900	commercial wrought P/M	25% cold rolled
Cu-21Ni-5Sn	–	cast and wrought	TM02
Cu-23Ni-5Co-8Sn	–	laboratory wrought P/M	25% cold rolled

(a)ASTM B601 temper designations.

Table 2—Composition and Melting Points of Solder

Solder Composition (wt-%)	Solidus Temperature (°C)	Liquidus Temperature (°C)
100% Sn	232	232
95Sn-5Sb	232	240
95Sn-5Ag	221	241
60Sn-40Pb	183	190
30Sn-70Pb	183	255
10Sn-90Pb	268	299
10Sn-88Pb-2Ag	268	302
5Sn-95Pb	305	312

characterize intermetallic compound formation on a number of copper-base alloys soldered with a variety of tin-containing solders and exposed at 150° to 250°C, in order to gain an understanding of the effects of base metal composition and solder alloy composition on the rate of intermetallic formation.

The exposure temperatures used in this study are generally higher than those used in previous studies of intermetallic formation in soldered copper-base alloys, and above the range of temperatures in which copper-base alloys have generally been used. Copper-base alloys have usually been limited by a lack of elevated temperature mechanical properties, and in particular, stress relaxation resistance, to a maximum temperature of 150°C for extended service. However, the development of spinodally hardened copper-nickel-tin alloys, such as Pfinodal®[1] alloy C72900, of composition Cu-15Ni-8Sn, has extended the maximum long-term temperature capability of high-strength, copper-base alloys to 225°C or higher (Ref. 16). The selection of solders suitable for use with a copper-base alloy at these higher temperatures requires that proper consideration be given to intermetallic formation at the interface between the solder and the base metal during long-term exposures.

Experimental Procedure

Materials

The copper-base alloys included in this study contain nickel and tin as major alloying additions, with nickel contents of 0 to 23 wt-% and tin contents of 0 to 8 wt-%. Beryllium-copper was also included as a material commonly used at 150°C. The majority of the alloys were of commercial manufacture including pure copper, Cu-5Sn-0.2P, Cu-1.9Be-0.4Co, Cu-9Ni-2Sn, Cu-9Ni-6Sn, Cu-15Ni-8Sn, and Cu-21Ni-5Sn. The Cu-15Ni-8Sn alloy is manufactured using a wrought powder metallurgy process (Ref. 17) and the other materials are manufactured by conventional casting and metalworking processes. Additional materials of compositions Cu-6Ni-4Sn, Cu-9Ni-6Sn, and Cu-23Ni-5Co-8Sn were prepared in experimental quantities by powder metallurgy techniques. Water-atomized powders were prepared from high-purity raw materials. The powder was roll compacted and sintered, and this material was brought to 100% density by additional cold rolling and annealing. The powder metallurgy processed copper-nickel-tin alloys are typically of very high purity. Iron is the major metallic impurity and is present at a level of 10 ppm or less. The wrought and cast copper-nickel-tin alloys contain 0.2 to 0.4% manganese and traces of silicon. The fabrication processes and material tempers are listed in Table 1.

The solders evaluated include high-tin content solders, high-lead content solders, and tin-lead, eutectic-forming solders. All of the base metal materials were evaluated with 95Sn-5Sb solder as representative of a high-tin solder frequently used in elevated temperature service conditions. All of the base metals were also evaluated with a 10Sn-90Pb solder representative of high-lead solders. A number of the base metals were also evaluated for intermetallic formation with 95Sn-5Ag and with 60Sn-40Pb solder. One of the alloys, Cu-15Ni-8Sn, was evaluated with four additional solder compositions, pure tin, 70Sn-30Pb, 10Sn-88Pb-2Ag, and 5Sn-95Pb, in order to further characterize the effect of solder composition on intermetallic formation. The solders were of commercial purity. The solder compositions included in this study are listed in Table 2 with the liquidus and solidus temperatures of each solder.

Sample Preparation

Specimens of each base metal alloy were prepared from strips of 0.18- to 0.25-mm (0.007- to 0.010-in.) thickness, 6-mm (0.25-in.) width, and 25-mm (1.0-in.) length. The copper-nickel-tin alloy strips of the laboratory-prepared materials were pickled in an aqueous solution of 5% sulfuric acid with 2% nitric acid for several seconds to clean surface oxides. (The Cu-15Ni-8Sn alloy was prepared both with and without prior pickling with identical results.) Each was bent to produce an L-shaped specimen which would retain a thick layer of solder on the top of the horizontal section when withdrawn from the solder bath. The specimens were ultrasonically cleaned in acetone and rinsed in methanol and deionized water. The specimens were dried and then dipped in an activated rosin flux (Multicore 366A). The solder was applied by dipping each specimen for 5 s into a ceramic crucible containing approximately 1 kg (2.2 lb) of solder maintained at a temperature 30°C (54°F) above the liquidus temperature of the solder. Solder temperature was monitored with a chromel-alumel thermocouple in a thin-wall alumina tube placed in the molten solder. Flux residues were removed from the specimens by ultrasonic cleaning in acetone and rinsing with methanol and deionized water.

The soldered specimens were suspended in air-circulating ovens at temperatures of 150°, 175°, 200° and 225°C (302°, 347°, 392° and 437°F), but not above the melting point (solidus temperature) of the solder. Specimens were removed for metallographic examination after 5, 20, 100, 500, 1500, and 2800 or 4000 h of continuous elevated temperature exposure. Additional testing was performed with 10Sn-90Pb solder at 250°C for times up to 500 h.

Intermetallic Characterization

Soldered specimens, both as-soldered and following elevated temperature exposure, were metallographically mounted and mechanically polished with 0.25 micron diamond abrasive. The intermetallic layers between the solder and the base metal were measured by optical microscopy at a magnification of 400X

[1]*Pfinodal® is a registered trademark of Pfizer, Inc.*

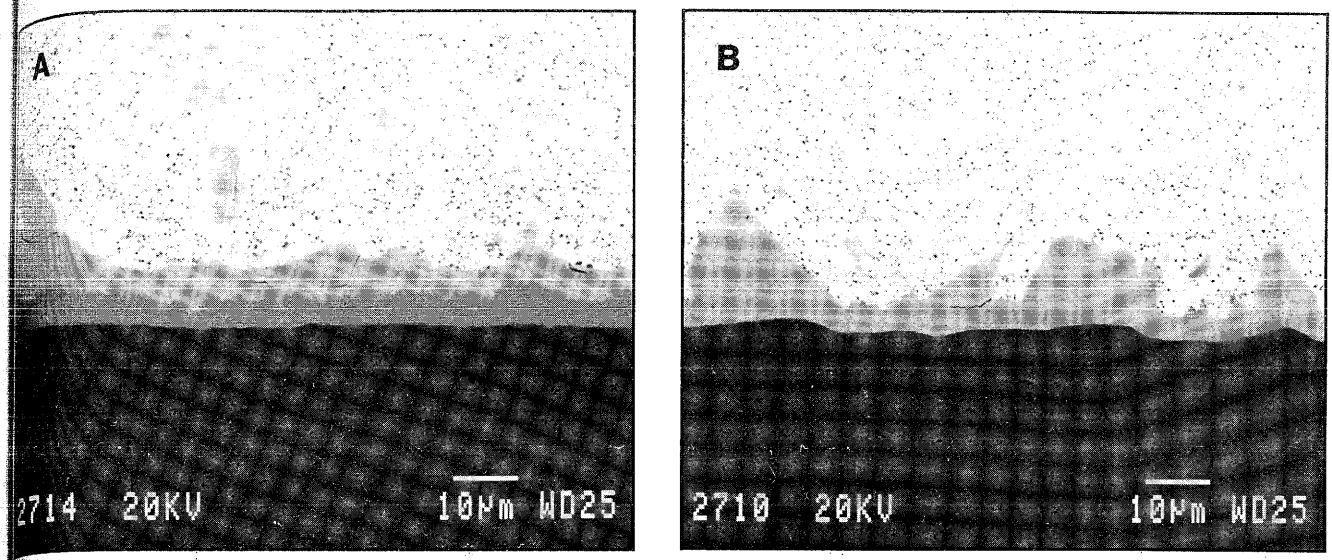

Fig. 1—Scanning electron micrographs of intermetallic layers formed after 4000 h at 150°C between 95Sn-5Sb and—A—pure copper; B—Cu-15Ni-8Sn

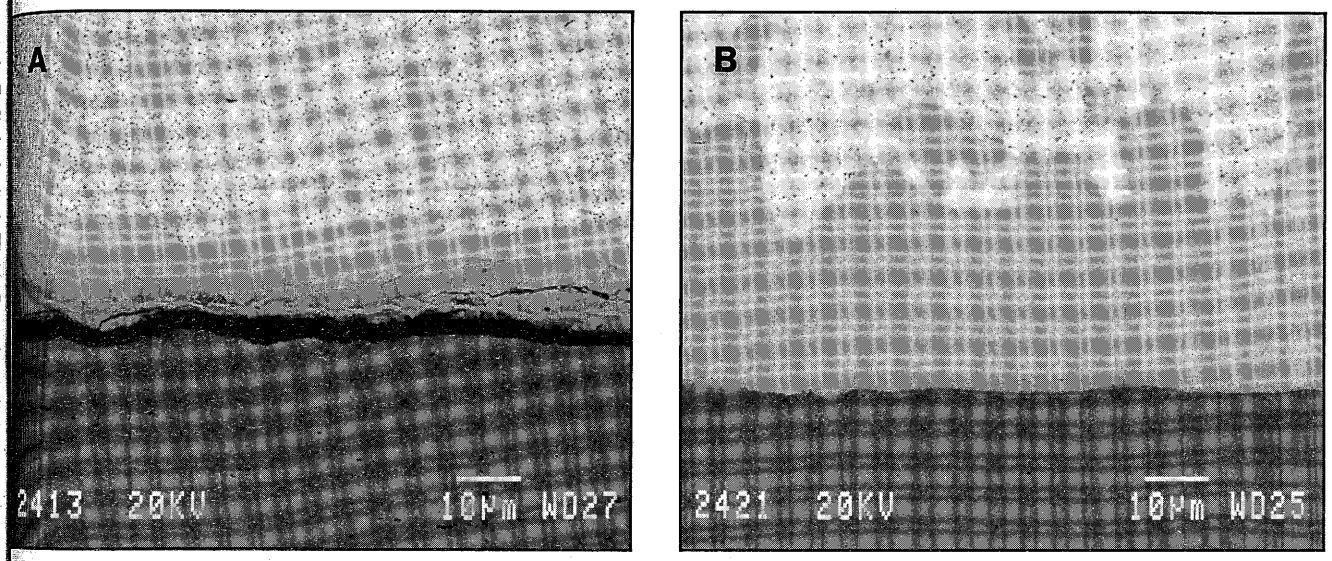

Fig. 2—Scanning electron micrographs of intermetallic layer formed after 4000 h at 150°C between 95Sn-5Sb and—A—Cu-1.9Be-0.4Co; B—Cu-9Ni-6Sn

sing a filar eyepiece with 2.5 microns/ vision. In general, the thickness of the ntermetallic layer was taken as the mean f five measurements. In some instances, e specimens were etched in an aque- us solution of 20 g/L $FeCl_3$, 40 g/L H_4NO_3 and 4 mL/L HNO_3, in order to nprove contrast between the interme- llic layer, base metal, and solder, as well s to show the grain boundaries of the ase metal. Additional layer thickness easurements were made using a JEOL A-840 scanning electron microscope at agnifications of 1000 to 5000 for layer icknesses of less than 5 microns.

Chemical analysis of the intermetallic ompounds was performed by scanning ectron microscopy using both energy nd wavelength dispersive x-ray analysis. hemical concentration variations within e intermetallic layer were characterized for a number of specimens by these methods.

The intermetallic layers formed on pure copper, Cu-9Ni-6Sn, and Cu-15Ni-8Sn were further characterized by x-ray diffraction analysis. Samples of base metal strip 25 mm (1 in.) square were dipped in pure molten tin, heated at 150°, 175° or 200°C to form intermetallic layers, and then immersed in 30% HNO_3 to remove the remaining surface layer of tin. In addition, powder samples were prepared by sintering of uncompacted pure copper, Cu-9Ni-6Sn, and Cu-15Ni-8Sn powder, infiltrating with molten tin, heating at 175° or 225°C to form the intermetallic layer and crushing and screening the material to −325 mesh powder. X-ray diffraction was performed using monochromated copper K_α radiation with 0.03-deg increments of 2 θ and a 2-s count time.

Results

Kinetics of Intermetallic Layer Growth

The analysis of intermetallic layer growth is concerned primarily with measurements of total intermetallic thickness. Scanning electron micrographs of some typical intermetallic layers formed on pure copper and Cu-15Ni-8Sn are shown in Fig. 1. Similar micrographs of Cu-9Ni-6Sn and Cu-1.9Be-0.4Co are shown in Fig. 2. It is apparent that the interface between the solder and the intermetallic layer is not planar, a result also found in previous studies on pure copper. (The small, dark particles in the solder are embedded diamond, an artifact of polishing.) The measurements of mean intermetallic layer thickness are found to be consistent with parabolic kinetics. As an

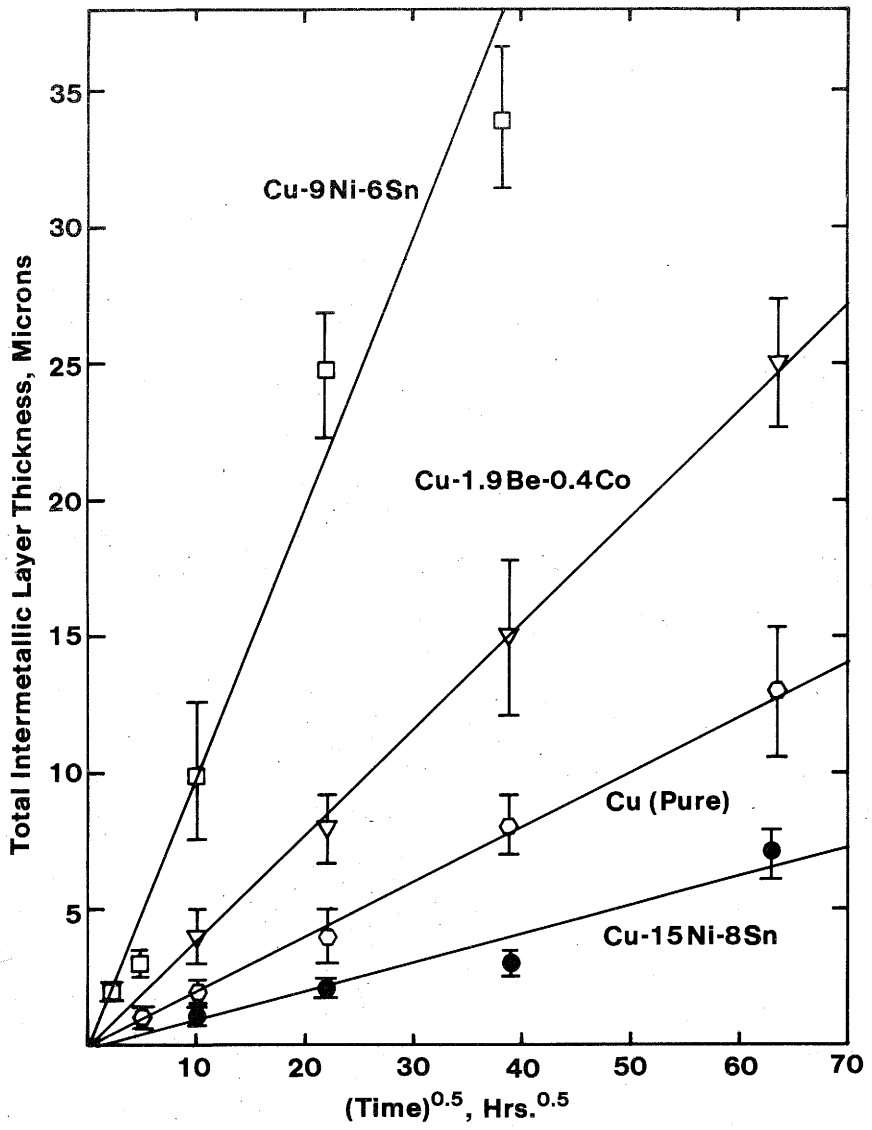

Fig. 3—Intermetallic layer thickness versus square root of exposure time for four copper-base alloys with 95Sn-5Sb solder at 150°C

example, the intermetallic layer thickness is plotted versus square root of exposure time in Fig. 3 for pure copper, Cu-1.9Be-0.4Co, Cu-9Ni-6Sn, and Cu-15Ni-8Sn soldered with 95Sn-5Sb and heated at 150°C for various times up to 4000 h. The standard deviation in the measured intermetallic layer thickness is also shown. The parabolic rate constant, k, in the equation relating intermetallic layer thickness, x, to exposure time, t, in the equation:

$$x = kt^{0.5}$$

is equivalent to the slope of the line giving the best fit to the data and is calculated for each condition using a statistical analysis described in the Appendix. The analysis used determines the value of the parabolic rate constant and also provides a measure of the uncertainty associated with that value.

The effect of base metal composition on intermetallic formation for materials soldered with 95Sn-5Sb solder is shown in Fig. 4 as a plot of the natural logarithm of the parabolic rate constant for intermetallic layer growth, as a function of nominal base metal nickel content (or nickel + cobalt content). Results are shown for exposure temperatures of 150°, 175°, and 200°C. The error bars correspond to plus or minus two standard deviations. At each temperature, there is a distinct maximum in intermetallic formation rate at a base metal nickel content of between 6 and 9%. Although the nickel and tin contents are not varied independently, it is clear that tin content of the base metal has relatively little effect on the intermetallic formation rate. Results for pure copper and Cu-5Sn-0.2P shown in Fig. 4 are equivalent within the indicated uncertainty in rate constant. The results for three materials containing a nominal nickel content of 9 wt-% are shown in Fig. 4. The differences between the three alloys with 9% nickel content are relatively small and not significant in all cases. Detailed analysis indicates that at each of the temperatures evaluated, the Cu-9Ni-2Sn alloy exhibits an intermetallic layer growth rate intermediate between that of the two Cu-9Ni-6Sn materials. These results show no evidence of intermetallic layer growth rate dependence on base metal tin content.

The results shown in Fig. 4 are regraphed as an Arrhenius plot in Fig. 5 to better illustrate the effect of temperature on intermetallic layer growth. (Error bars are omitted for the sake of clarity.) The slope of each curve is proportional to the activation energy for intermetallic layer growth. The copper alloys can be divided into three groups on the basis of activation energy behavior. The alloys which do not contain nickel have a constant activation energy for intermetallic layer growth over the temperature range of 150° to 200°C. The four alloys containing 6 to 9% nickel all show a lower activation energy for the temperature interval of 175° to 200°C, as compared to the temperature interval of 150° to 175°C. The three alloys containing 15% nickel or more exhibit a substantially higher activation energy for the temperature interval of 175° to 200°C, as compared to the interval 150° to 175°C. The activation energies for pure copper and the nickel-free alloys are in the range of 8800 to 12,600 cal/mol. The activation energies for the nickel-containing alloys range from 9900 to 35,000 cal/mol.

The parabolic rate constants for intermetallic formation of a smaller group of base metals soldered with another high-tin content solder, 95Sn-5Ag, are shown as an Arrhenius plot in Fig. 6. The behavior of the activation energy is very similar to that seen with 95Sn-5Sb solder. The dependence of the parabolic rate constant on nickel content of the base metal for the 95Sn-5Ag solder is also similar to that for 95Sn-5Sb solder. At the 150°C exposure temperature, the rate constant is greatest at a base metal nickel content of 9%, smaller at a nickel content of 0% and smallest at a 15% nickel content. At 175°C, the rate constant is greatest at a 9% base metal nickel content and similar in value for the alloys containing 0% and 15% nickel. At 200°C, the results for the 95Sn-5Ag solder differ from those obtained with the 95Sn-5Sb solder in that the rate constant for Cu-15Ni-8Sn is significantly higher and is equivalent to the rate constant for Cu-9Ni-6Sn.

The results of intermetallic layer growth obtained with 60Sn-40Pb solder are shown in Fig. 7 for exposure temperatures of 150° and 175°C. The dependence of intermetallic formation rate on base metal nickel content is consistent with that of the high-tin content solders. The rate constant is largest at a nickel content of 9%, much lower at 0%, and lowest at 15%. At 175°C, the rate con-

indicates that
res evaluated,
its an interme-
intermediate
o Cu-9Ni-6Sn
how no evi-
r growth rate
l tin content.
Fig. 4 are
lot in Fig. 5 to
f temperature
th. (Error bars
f clarity.) The
ortional to the
rmetallic layer
can be divided
asis of activa-
alloys which
/e a constant
metallic layer
ture range of
oys containing
wer activation
re interval of
pared to the
0° to 175°C.
15% nickel or
higher activa-
rature interval
pared to the
he activation
nd the nickel-
e of 8800 to
ation energies
alloys range
ol.

ants for inter-
aller group of
another high-
g, are shown
5. The behav-
is very similar
b solder. The
olic rate con-
he base metal
also similar to
At the 150°C
rate constant
nickel content
ontent of 0%
el content. At
greatest at a
nt and similar
aining 0% and
results for the
from those
solder in that
5Ni-8Sn is sig-
ivalent to the
n.

metallic layer
n-40Pb solder
sure temper-
. The depen-
ation rate on
is consistent
ntent solders.
t at a nickel
r at 0%, and
the rate con-

ant is highest at 9% nickel and lowest at
% nickel. The activation energies for
termetallic layer growth for the three
oys without a nickel addition are in the
nge of 14,000 to 16,000 cal/mol. The
tivation energy for intermetallic layer
owth for the Cu-15Ni-8Sn alloy is
,000 cal/mol. These values are mark-
ly higher than those for the same alloys
dered with the high-tin content solder
easured over the same temperature
erval.

The results of measurements of para-
olic rate constants for material soldered
ith the high-lead solder, 10Sn-90Pb, are
ted in Table 3 for temperatures of
0°, 225° and 250°C. At the 200°C test
mperature, there is no systematic varia-
on in the rate constant with base metal
mposition. The uncertainty limits are
nerally larger than those obtained for
e higher tin content solders. At 225°C,
e data suggest that the higher nickel
ntent materials, Cu-21Ni-5Sn and Cu-
Ni-8Sn-5Co, form intermetallic layers
ss rapidly than lower nickel content
aterials. At 250°C, the parabolic rate
nstants, determined for exposure times
up to 500 h, indicate a distinctly lower
te of intermetallic formation in the high-
nickel content materials. At all temper-
ures, the variations in intermetallic for-
ation rate with base metal composition
btained with the 10Sn-90Pb solder are
all in comparison with those obtained
ith higher tin content solders.

The effects of solder composition on
termetallic layer growth rate for one
rticular base metal alloy, Cu-15Ni-8Sn,
e shown in Fig. 8. The results include
se for the four solders previously
scribed (error bars omitted), as well as
ur additional solders, pure tin, 30Sn-
0Pb, 10Sn-88Pb-2Ag, and 5Sn-95Pb. The
ree high-tin content solders show simi-
r intermetallic growth rate behavior,
ith the parabolic rate constant for pure
in intermediate between the somewhat
gher rate for 95Sn-5Ag and the some-
hat lower rate for 95Sn-5Sb. The inter-
etallic formation rates for the two
utectic-containing solders, 30Sn-70Pb
d 60Sn-40Pb, are virtually identical
spite the wide variation in tin contents
the solders. A comparison of the three
gh-lead content solders indicates that
e 5Sn-95Pb solder forms intermetallic
mpounds at a much lower rate than
e 10Sn-90Pb solder. The 10Sn-88Pb-
Ag exhibits significantly lower rate con-
nts than the binary solder alloy with
e same nominal tin content.

The effects of solder composition on
termetallic formation rate for base met-
compositions other than Cu-15Ni-8Sn
ere not investigated in detail. A com-
rison of the data for the two high-tin
lders in Figs. 5 and 6 with the near-
utectic 60Sn-40Pb solder in Fig. 7 indi-
tes that the intermetallic formation

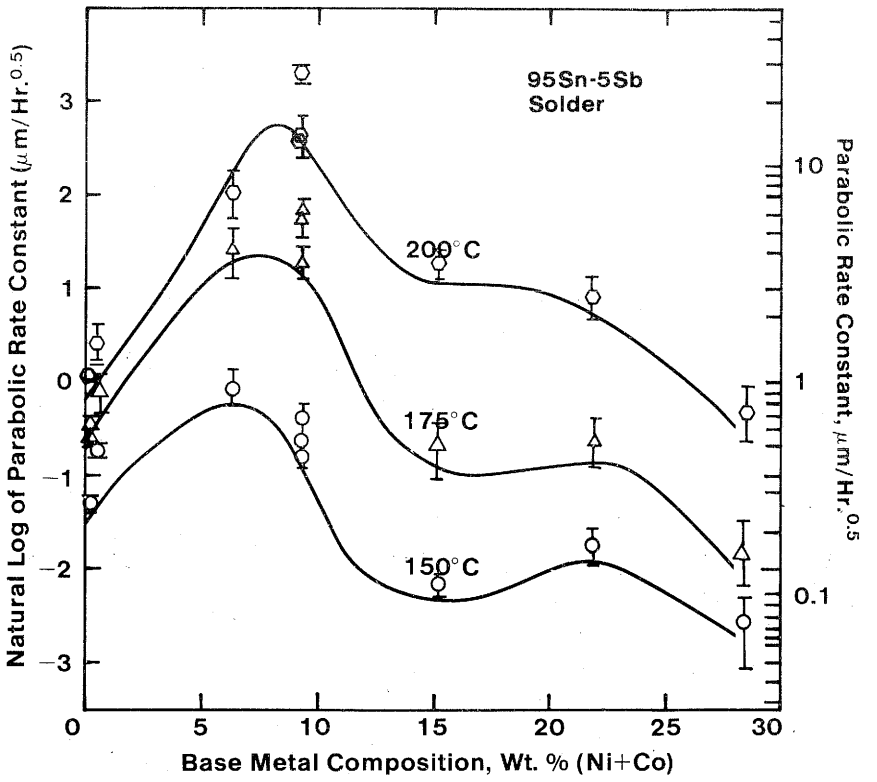

Fig. 4—Dependence of intermetallic formation rate on base metal composition for 95Sn-5Sb solder at 150°, 175° and 200°C

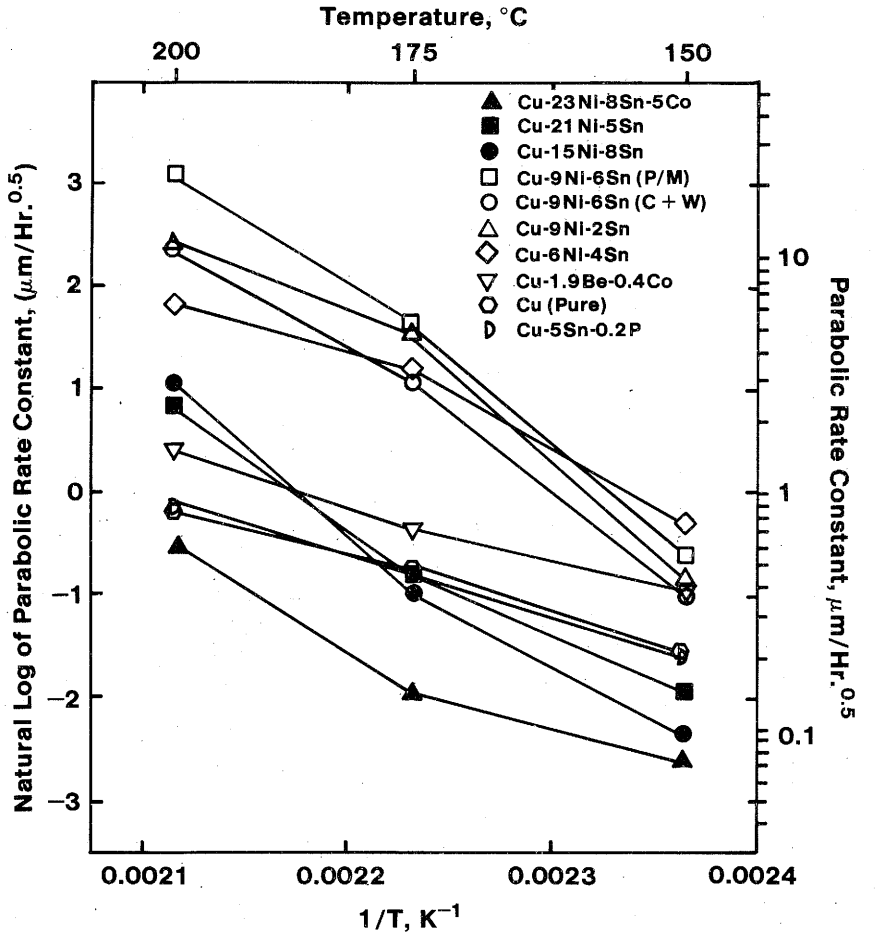

Fig. 5—Arrhenius plot for intermetallic layer growth for copper-base alloys soldered with 95Sn-5Sb

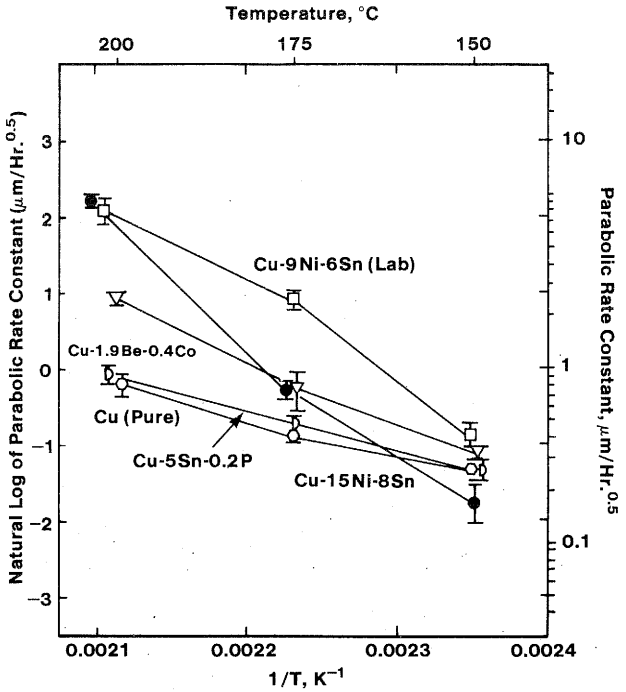

Fig. 6—Arrhenius plot for intermetallic layer growth for copper-base alloys soldered with 95Sn-5Ag

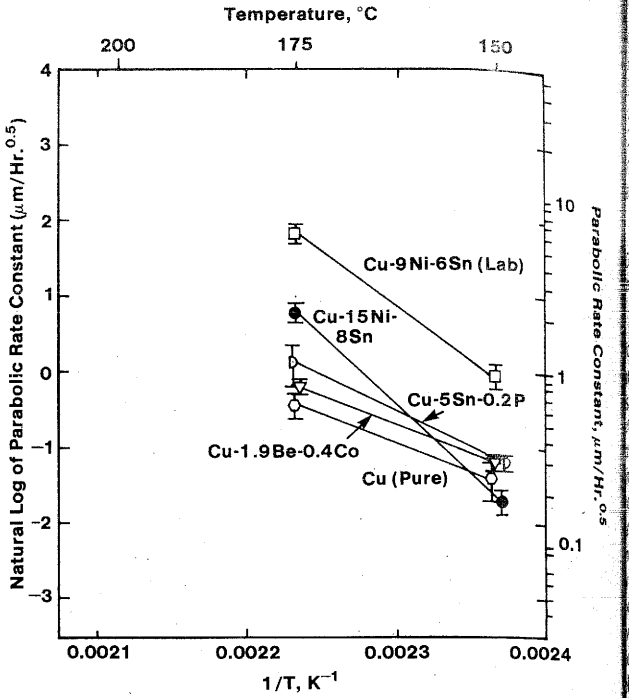

Fig. 7—Arrhenius plot for intermetallic layer growth for copper-base alloys soldered with 60Sn-40Pb

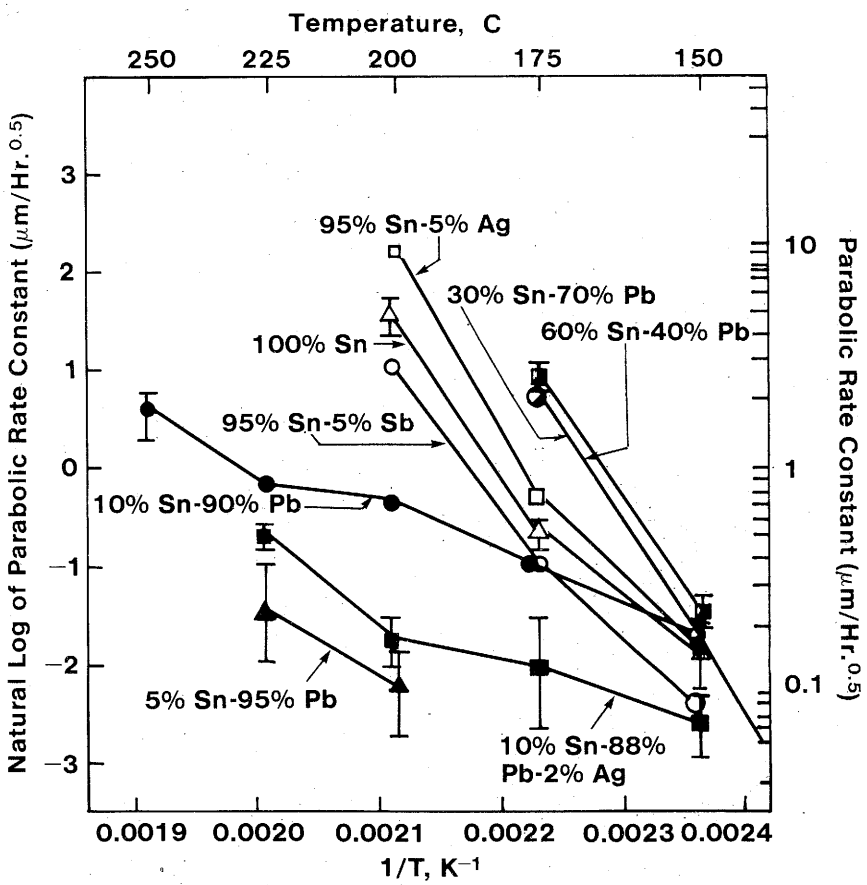

Fig. 8—Arrhenius plot for intermetallic layer growth for Cu-15Ni-8Sn with various solders

rates at 150°C for pure copper, Cu-5Sn-0.2P and Cu-1.9Be-0.4Co are similar for all three solders. In contrast, Cu-9Ni-6Sn at 150°C exhibits a parabolic rate constant for 60Sn-40Pb solder which is approximately twice that for the high-tin content solders. At 175°C, all of the base metal alloys exhibit higher rate constants with the 60Sn-40Pb solder than with the high-tin content solders, and the difference is largest in the case of Cu-15Ni-8Sn. The lower rate constants for 10Sn-88Pb-2Ag solder as compared to 10Sn-90Pb solder for Cu-15Ni-8Sn are also observed for pure copper and Cu-5Sn-0.2P in limited testing at 225°C. For pure copper, the rate constant is 1.08 $\mu m/\sqrt{h}$ for 10Sn-88Pb-2Ag, as compared to 1.31 $\mu m/\sqrt{h}$ for 10Sn-90Pb. For Cu-5Sn-0.2P, the rate constant is 0.81 $\mu m/\sqrt{h}$ for 10Sn-88Pb-2Ag, as compared to 1.17 $\mu m/\sqrt{h}$ for 10Sn-90Pb.

The thickness measurements made for Cu_3Sn layers formed on pure copper and Cu-5Sn-0.2P are summarized in Table 4. The results are listed as the ratio of the mean Cu_3Sn layer thickness to the total intermetallic layer thickness. The ratio does vary with exposure time initially in some instances, but remains relatively constant with time after a total intermetallic layer thickness of 5 to 10 microns is obtained. The ratio values listed are the mean of the long time measurements for which the total intermetallic layer thickness is 10 microns or more. The pure copper and Cu-5Sn-0.2P exhibit similar behavior, and the differences between the two are likely within the experimental error. The 95Sn-5Sb and 95Sn-5Ag sol-

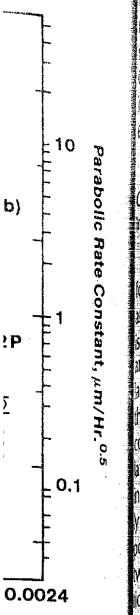

copper-base

...ers have ratios of 0.3 to 0.5 and the ...0Sn-40Pb solder has ratios of 0.25 to ...3. The 10Sn-90Pb solder shows high ...atios at 200°C and above, indicating Cu_3Sn has become the predominant ...ntermetallic layer formed at the higher ...xposure temperatures.

Composition and Structure of Intermetallic Compounds

Although the intermetallic compounds ...ormed by the nickel-containing alloys ...re all characterized as $(Cu,Ni)_6Sn_5$, there ...s considerable variation in the copper ...nd nickel contents of the intermetallic ...ayer formed with each alloy. In addition, ...here may be considerable variation in ...omposition within a single intermetallic ...ayer. These compositional changes with- ...n certain intermetallic layers can be readi- ...y observed by optical metallography of ...olished cross-sections and appear as ...wo distinct layers of intermetallic forma- ...on with distinctly different contrast. The ...henomenon is prominent in Cu-15Ni- ...Sn and Cu-21Ni-5Sn alloys soldered with ...5Sn-5Sb or 95Sn-5Ag solder and ...xposed at 150° or 175°C. At 200°C, the ...ntermetallic layer is uniform in appear- ...nce. A composition profile across the ...ntermetallic zone formed between Cu- ...5Ni-8Sn and 95Sn-5Sb solder at 175°C ...fter 500 h of exposure is plotted in Fig. ...9. The intermetallic zone consists of two ...egions of approximately equal thickness. ...he region adjacent to the Cu-15Ni-8Sn ...ase metal has a nickel content of ...etween 11 and 12 wt-%. The region ...djacent to the solder has a nickel con- ...ent between 3 and 5 wt-%. The compo- ...itions of the two regions can be approx- ...mated as $(Cu_4Ni_2)Sn_5$ and $(Cu_5Ni_1)Sn_5$, ...espectively. Similar profiles obtained for ...200°C exposure indicate a uniform ...omposition across the intermetallic lay- ...r. The ratio of nickel to copper in the ...ntermetallic layer formed at 200°C has a ...onstant value across the entire interme- ...allic layer of 0.21, the same as that of the ...u-15Ni-8Sn base metal. The results of ...EM/EDAX analysis of intermetallic com- ...ositions are summarized in Table 5 for a ...umber of conditions in which two dis- ...inct layers of the $(Cu,Ni)_6Sn_5$ intermetallic ...ayer are observed. This type of double ...ayer is observed with high-tin solders ...nd only at 150°C for Cu-9Ni-6Sn and at ...50° and 175°C for Cu-15Ni-8Sn and ...u-21Ni-5Sn. The composition profile of ...u-9Ni-6Sn soldered with 95Sn-5Sb and ...eated at 150°C for 4000 h is shown in ...g. 10. There is a narrow intermetallic ...yer, 3 microns in thickness, with an ...evated nickel content, located adjacent ...o the base metal. The Cu-15Ni-8Sn alloy ...oldered with high-lead content solders ...oduces localized intermetallic regions ...f high-nickel content near the interface ...ith the base metal, during exposure at

Table 3—Intermetallic Formation Rates for Copper Alloys Soldered with 10Sn-90Pb Solder

Base Metal	Parabolic Rate Constant at Indicated Exposure Temperature ($\mu m/\sqrt{h}$) 200°C	225°C	250°C
Cu (Pure)	0.73 ± 0.12	1.31 ± 0.18	1.8 ± 0.9
Cu-5Sn-0.2P	0.68 ± 0.08	1.17 ± 0.16	–
Cu-6Ni-4Sn	0.80 ± 0.32	1.95 ± 1.12	2.08 ± 0.27
Cu-9Ni-6Sn (P/M)	0.44 ± 0.14	0.93 ± 0.30	2.38 ± 0.64
Cu-9Ni-6Sn (Cast and Wrought)	0.77 ± 0.25	1.20 ± 0.60	–
Cu-9Ni-2Sn	0.36 ± 0.07	0.61 ± 0.21	–
Cu-15Ni-8Sn	0.71 ± 0.12	0.98 ± 0.29	1.82 ± 0.90
Cu-21Ni-5Sn	0.43 ± 0.15	0.67 ± 0.16	1.01 ± 0.18
Cu-23Ni-8Sn-5Co	0.60 ± 0.11	0.55 ± 0.13	0.73 ± 0.23

Table 4—Relative Thickness of the Cu_3Sn Intermetallic Layer

Alloy	Solder	Ratio of Cu_3Sn Layer Thickness to Total Intermetallic Layer Thickness at Indicated Temperature (°C) 150	175	200	225	250
Pure Cu	95Sn-5Sb	0.38	0.42	0.43		
	95Sn-5Ag	0.32	0.33	0.38		
	60Sn-40Pb	0.30	0.30			
	10Sn-90Pb	0.46	0.54	0.68	0.50	0.73
Cu-5Sn-0.2P	95Sn-5Sb	0.30	0.40	0.50		
	95Sn-5Ag	0.30	0.45	0.46		
	60Sn-40Pb	0.25	0.30			
	10Sn-90Pb	0.36	0.44	0.65	0.77	0.77

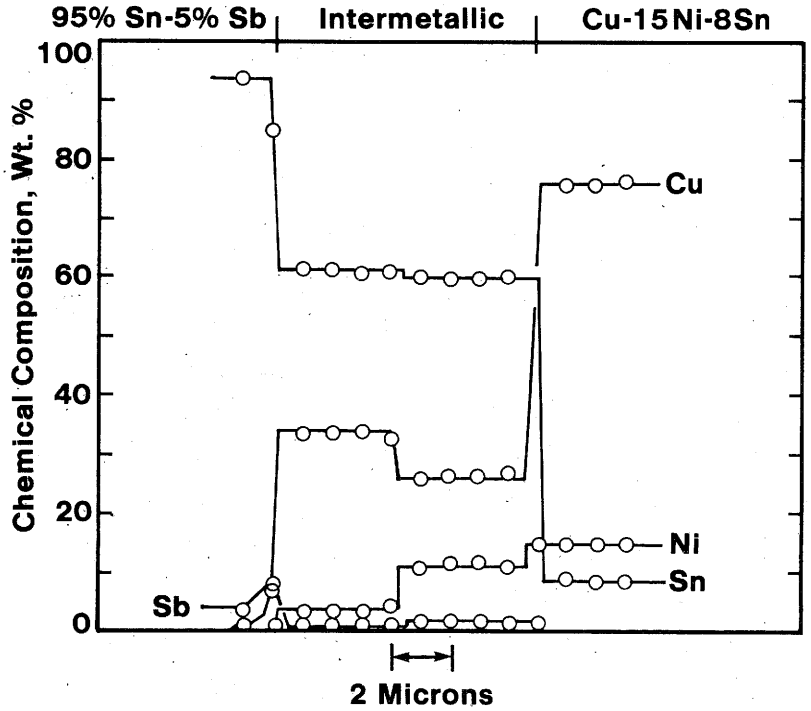

Fig. 9—Composition profile of the intermetallic compound formed between Cu-15Ni-8Sn and 95Sn-5Sb solder after 500 h at 175°C

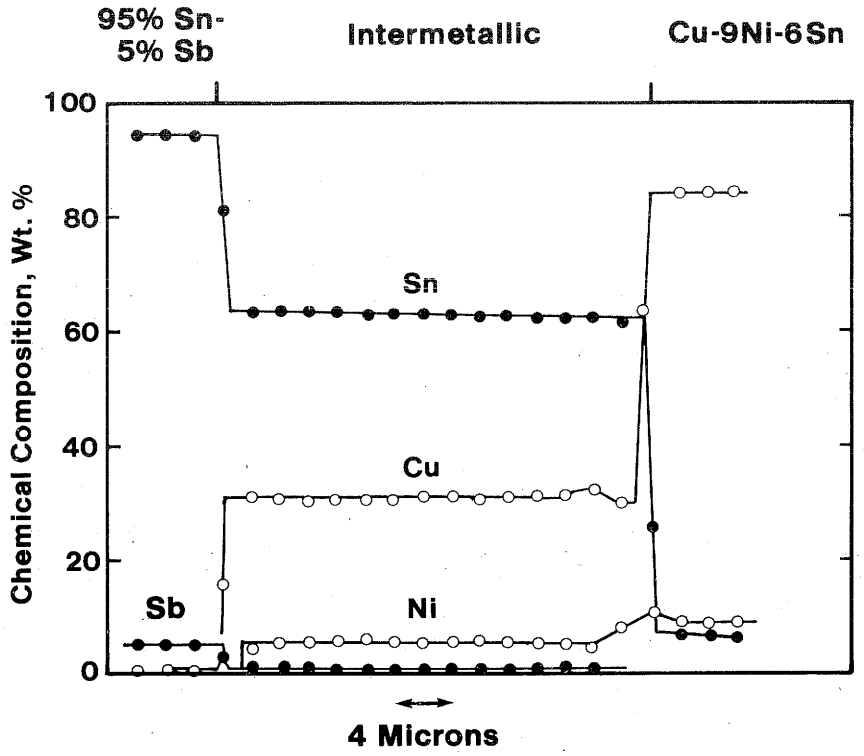

Fig. 10—Composition profile of the intermetallic compound formed between Cu-9Ni-6Sn and 95Sn-5Sb solder after 4000 h at 150°C

200° and 225°C. Changes in contrast in the intermetallic layer formed on Cu-1.9Be-0.4Co are found to correlate qualitatively with changes in tin concentration as measured by SEM/EDAX, although no quantitative analyses were performed.

In addition to the segregation within the intermetallic, chemical segregation is also observed in the solder and at the solder/intermetallic interface. In the case of 60Sn-40Pb solder, the tin-depleted zone of the solder is clearly seen as a zone depleted of eutectic adjacent to the intermetallic layer in Fig. 11. The 10Sn-90Pb alloy exhibits a tin-depleted region with a tin content of 4% adjacent to the intermetallic interface formed with Cu-15Ni-8Sn at 200°C. In the case of the

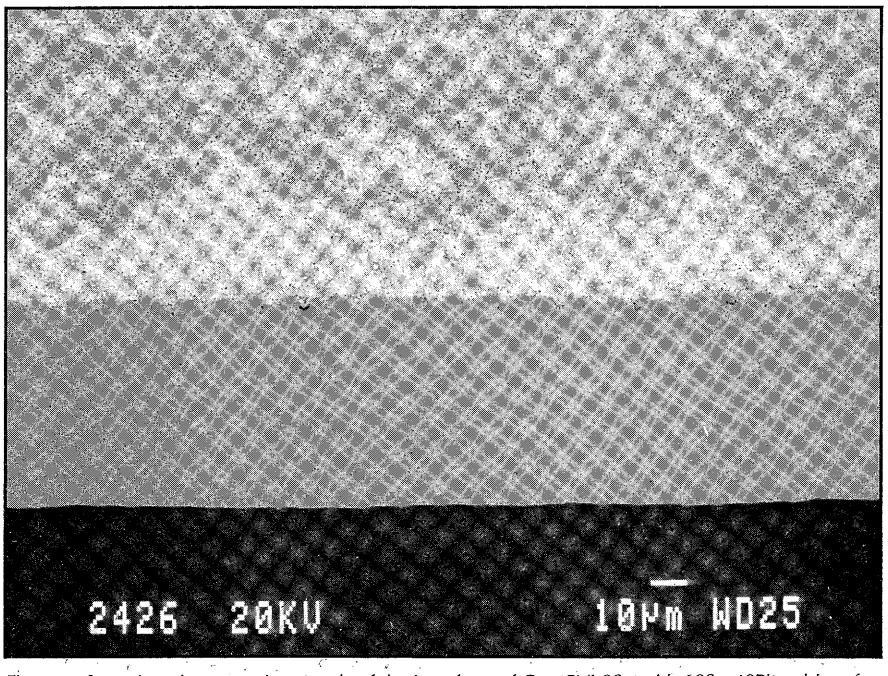

Fig. 11—Scanning electron micrograph of the interface of Cu-15Ni-8Sn with 60Sn-40Pb solder after 500 h at 175°C

10Sn-88Pb-2Ag solder, the silver reacts to form particles of Ag_3Sn intermetallic compound, which may be observed at the interface of the solder and the $(Cu,Ni)_6Sn_5$ intermetallic layer. Antimony in the 95Sn-5Sb solder is partially rejected by the solder at the interface with the intermetallic formation, as can be seen in Fig. 9. At very high rates of intermetallic formation, such as for Cu-9Ni-6Sn, substantial quantities of antimony can accumulate at the solder interface and have been observed as a continuous layer of the β phase, of compositions 57Sn-43Sb by weight, at the interface of Cu-9Ni-6Sn with 95Sn-5Sb heated at 175°C for 1500 h.

The morphology of the intermetallic layers vary from planar interfaces with layers of uniform thickness to wavy or dendritic interfaces which may appear as regions that in a cross-section seem not to be connected. The nonuniform morphologies cannot be readily associated with any particular solders or base metal compositions. The nonuniformity tends to increase with increasing exposure time and mean layer thickness. Another feature is the tendency for the intermetallic layer to crack and to debond from the base metal during intermetallic formation. The detachment of the intermetallic layer by fracture near the interface with the base metal depends on the geometry of the solder interface, and also appears to be related to solder composition and base metal composition. The high-lead solders tend to produce intermetallic layers that are more prone to interfacial fracture than do high-tin content solders. Of the base metals evaluated, the Cu-1.9Be-0.4Co is significantly more prone to interfacial fracture than any other base metal studied. This behavior is typified by the micrograph shown in Fig. 2. The combination of Cu-1.9Be-0.4Co and 10Sn-90Pb solder is very susceptible to interfacial fracture. Reliable parabolic rate constants could not be generated for this material combination, due to excessive interfacial fracture.

Although no measurements were made using Kirkendall markers, it is possible to estimate the location of the original interface between the solder and the base metal on a number of specimens by cold rolling a pure tin strip between two strips of copper-nickel-tin alloy. After heating of Cu-6Ni-4Sn and Cu-9Ni-6Sn specimens at 175°C and Cu-15Ni-8Sn at 200°C, cross-sections show regions in which intermetallic layer growth has occurred between two adjacent regions in which no intermetallic compound has formed at the boundary, presumably due to a thin oxide at the interface. The location of the original interface can be estimated with reasonable accuracy, and in all cases approximately equ

quantities of intermetallic compounds are found to form on both sides of the boundary. These results indicate that under these conditions the diffusion constants for copper, nickel and tin in the η phase are all of the same order of magnitude.

X-ray diffraction analysis of both intermetallic surfaces from which the overlying solder was chemically stripped and intermetallic powders prepared by reaction of tin with copper-nickel-tin alloy powders reveal only the presence of η-$(Cu,Ni)_6Sn_5$, a hexagonal structure. One exception to this is that a trace of the ε-Cu_3Sn phase is detected by x-ray diffraction for Cu-9Ni-6Sn and Cu-15Ni-8Sn powder infiltrated with tin and heated at 225°C for 500 h. Unlike the specimens used for layer growth rate measurements, the tin is completely consumed by the formation of η phase in this process. The lattice parameters of the η-Cu_6Sn_5 phase obtained from powder samples for pure copper are $c_o = 5.100 +/- 0.006$ and $a_o = 4.188 +/- 0.004$ Å. The lattice variables for the η phase formed with Cu-15Ni-8Sn alloy at 175° and 225°C are $c_o = 5.105 +/- 0.003$ Å and $a_o = 4.210 +/- 0.003$ Å. The η phase formed with Cu-9Ni-6Sn at 175°C has lattice variables similar to those of the η phase formed with Cu-15Ni-8Sn. The Cu-Ni-6Sn reacted at 225°C has η lattice variables similar to those obtained by reaction with pure copper.

Discussion

Base Metal Composition Effects

The major variables evaluated in this study of intermetallic layer growth are the composition of the base metal, the composition of the solder, and the exposure temperature. Although the effects of these variables are interrelated to a large extent, the following discussion treats the effects of each variable in order, as much as is practical. The effects of base metal composition of the copper-based alloys in this study can be separated into those conditions in which base metal composition significantly affects intermetallic layer growth and those in which the effect is small. Under conditions in which intermetallic formation rate is sensitive to base metal composition, such as for the solders containing 30% tin or more at exposure temperatures of 150° to 200°C, and for 10Sn-90Pb solder at 250°C, it is postulated that the rate-controlling step is the layer growth is diffusion through the intermetallic layer. Under conditions in which intermetallic formation is not sensitive to base metal composition, such as for solders containing 10% tin or less at exposure temperature of 200°C or less, it is postulated that the rate-controlling step is diffusion of tin through the solder. The effect of nickel content of copper-base alloys on the rate of intermetallic formation with tin-containing solders has not been studied previously in any detail. The only such work of which the author is aware is the unpublished results of Fister and Breedis (Ref. 18) on binary copper-nickel alloys containing 0 to 20% nickel, which were electroplated with a 5-micron-thick coating of 60Sn-40Pb solder and exposed at 150°C for 96 h. Their results show a maximum in intermetallic formation rate at a nickel content of 9 wt-% and are in excellent quantitative agreement with the results obtained in this study for 60Sn-40Pb solder with pure copper, Cu-9Ni-6Sn, and Cu-15Ni-8Sn.

The variation in intermetallic formation rate with base metal composition can be related to the changes in intermetallic composition. It is likely that these changes can affect the atomic structure of the η-Cu_6Sn_5 phase with substantial effect on diffusion in this intermetallic phase. The rapid diffusion in the copper-tin intermetallic formation has been related to structural vacancies and ordering within these phases. Alloying of nickel with the Cu_6Sn_5 intermetallic compound may have important effects on the concentration of structural vacancies which can be detected by changes in relative intensity of x-ray diffraction peaks. X-ray diffraction peak intensities of intermetallic powder formed on Cu-15Ni-8Sn powder at 175°C do exhibit significant differences from those formed on Cu-9Ni-6Sn or pure copper, as well as those formed on Cu-15Ni-8Sn at 225°C. The η-Cu_6Sn_5 phase is closely related to the B_8 structure type which has copper at the 0, 0, 0 and 0, 0, ½ lattice sites and tin at the ⅓, ⅔, ¾, and ⅔, ⅓, ¼ sites. It is possible that diffusion in this structure is sensitive to the degree of occupancy of the open regions within the lattice centered at ⅓, ⅔, ¼ and ⅔, ⅓, ¾ lattice positions. Unfortunately, the variation in x-ray diffraction peak intensities, with nickel content of the alloy powder, could not be consistently related to changes in occupancy of these sites. At least part of the difficulty in this analysis is that the intermetallic compound formed on each powder particle, rather than being uniform in composition, has a double layered structure similar to that formed on the soldered strip samples. A structural analysis of vacancy concentrations and ordering as a function of composition of the η-$(Cu,Ni)_6Sn_5$ phase is necessary to explain the effects of base metal composition on intermetallic layer growth seen in this study, since these effects can have large effects on diffusion in intermetallic compounds (Ref. 19).

The results of this study show a definite relationship between the segregation of nickel within the intermetallic layer and the kinetics of intermetallic layer growth. For the Cu-15Ni-8Sn alloy, relatively low intermetallic formation rates are obtained at temperatures of up to 175°C with the high-tin content solders and at 150°C with the 60Sn-40Pb solder, under conditions in which two distinct intermetallic regions with differing nickel content are formed. The absence of nickel segregation in the intermetallic layer at slightly higher temperature is associated with much higher rates of intermetallic formation. Similar behavior is observed for Cu-9Ni-6Sn with high-tin content solders at 150°C. In the case of Cu-15Ni-8Sn soldered with 95Sn-5Sb, there is a substantially lower activation energy for layer growth associated with the temperature interval in which nickel segregation occurs than there is for the temperature range in which no nickel segregation occurs. Additional experiments at temperatures below 150°C are required to establish whether the same relationship exists for Cu-15Ni-8Sn soldered with 60Sn-40Pb, and Cu-9Ni-6Sn soldered with 95Sn-5Sb.

The segregation behavior of nickel within the intermetallic layer cannot be explained simply by differences in diffusivity of copper and nickel within the intermetallic layer. An increase in nickel content of the intermetallic layer adjacent to the interface with the base metal would result from a lower diffusion coefficient of nickel, as compared to copper, in the intermetallic layer. However, this would in general be seen as a continuous decrease in nickel content across the intermetallic layer. The observation of a distinct boundary between layers of differing nickel contents suggests that at 175°C and below, the intermetallic compositions of nickel contents between about 5 and 10% nickel are thermodynamically less stable than those of higher and lower nickel content. The observed formation of an intermetallic layer with a nickel-to-copper ratio higher than that of the base metal alloy is sufficient to explain a reduction in the intermetallic layer growth rate. The high-nickel content intermetallic layer has a low rate of growth, which can be associated with the low rate of intermetallic layer growth on high-nickel content base metals. The rate of growth of this layer limits the rate of growth of the low-nickel content layer, in that copper must be transported through the high-nickel content intermetallic layer before reacting to form an additional intermetallic layer of low-nickel content. Experimental results shown in Table 4 indicate that the nickel-to-copper ratios in the low-nickel content layer are in the range of 0.09 to 0.16, which is similar to that obtained for much thicker intermetallic layers of uniform composition produced under the same exposure conditions on base metal alloys with 9% nickel. Transport through the low-nickel content

layer is, therefore, not a rate-limiting process. Although the observed nickel segregation in the intermetallic layer does account for the associated low-rate constants and activation energies for intermetallic layer growth, further study is required to determine the cause of the segregation itself.

Comparison of the intermetallic layer growth rates of base metal alloys with the same nickel content but with different tin contents shows little or no effect of variations in tin content of several percent. This result is consistent with a most simple model of intermetallic layer growth in a binary system with a constant diffusion coefficient of tin in Cu_6Sn_5 (or $[Cu,Ni]_6Sn_5$), and fixed intermetallic tin compositions at the solder and base metal interfaces of C_1 and C_2, respectively. Equating the flux of tin through the intermetallic layer with its consumption to form an intermetallic composition at the intermetallic/base metal interface and assuming no significant diffusion in the base metal having tin content C_3, no volume changes and a limited composition range of the intermetallic layer (*i.e.*, $[C_1-C_2] \ll [C_2-C_3]$), the compositions can be expressed as mole fractions resulting in an expression for intermetallic layer thickness, x, of

$$\frac{x}{t^{1/2}} = \left[\frac{2\,D\,(C_1-C_2)\,(1-C_3)}{(C_2-C_3)(1-C_2)}\right]^{1/2}$$

in which D is the diffusivity of tin in the intermetallic layer and t is the exposure time.

An increase in C_3, the base metal tin content, from 0 to 5 wt-% produces an increase in the parabolic rate constant of less than 2%, which is substantially less than the uncertainty in experimental measurement of the rate constant. The same result is obtained by a somewhat different means if copper is assumed to be the diffusing species. Although more complex models could be used to more accurately model the intermetallic layer growth, including the presence of the ϵ-Cu_3Sn intermetallic compound, this would not alter the conclusion that the variation in tin contents of the base metal alloys in this study cannot be expected to have any measurable effect on the rates of intermetallic layer growth.

The nickel content of the base metal alloy, in addition to its effect on the rate of intermetallic formation, also affects the formation of the ϵ intermetallic phase. The absence of an intermetallic ϵ phase layer on any of the soldered nickel-containing specimens following exposures at 150° to 250°C can be the result of either thermodynamic or kinetic effects of nickel. A large decrease in diffusivity in the ϵ phase with increased nickel content could result in very small layer thicknesses which are not detected.

Table 5—Composition Analysis of Intermetallic Layers Showing Nickel Segregation

Temp./ Time	Base Metal/ Solder	Intermetallic Thickness (μm)	Composition of Zones Adjacent to Base Metal or Solder, Composition (wt-%) Cu	Ni	Sn	Other
150°C/ 1500 h	Cu-15Ni-8Sn/ 95Sn-5Sb	3 3	28	12 Not measured	61	1 Sb
175°C/ 1500 h	Cu-15Ni-8Sn/ 95Sn-5Sb	8 9	27 35	11 3	61 61	1 Sb 1 Sb
150°C/ 1500 h	Cu-15Ni-8Sn/ 95Sn-5Ag	3 5	30 35	10 3	60 62	1 Sb
175°C/ 1500 h	Cu-15Ni-8Sn/ Pure tin	10 10	29 34	10 4	61 62	
175°C/ 1500 h	Cu-15Ni-8Sn/ 60Sn-40Pb	2 55	26 32	13 6	61 62	
150°C/ 4000 h	Cu-9Ni-6Sn/ 95Sn-5Sb	4 26	30 31	8 6	61 63	1 Sb 1 Sb
175°C/ 1500 h	Cu-21Ni-5Sn/ 95Sn-5Sb/	8 6	27 30	10 5	61 64	1 Sb 1 Sb
225°C/ 500 h	Cu-15Ni-8Sn/ 10Sn-90Pb	4 20	24 35	18 4	58 59	1 Pb 1 Pb

Alternatively, the ϵ phase may be thermodynamically less stable in the presence of nickel contents above a few percent. The x-ray diffraction analyses of tin-infiltrated copper-nickel-tin powders exposed at 225°C does show traces of ϵ under conditions in which layer growth is terminated by the complete consumption of tin by the η phase. These results, under conditions which are a closer approach to equilibrium, indicate that the ϵ phase is not completely unstable in the presence of these low-nickel contents. In the absence of phase diagram data for the copper-nickel-tin system at these temperatures, it is not possible to determine the cause for the absence of the ϵ intermetallic formation with the nickel-containing copper-base alloys in this study.

Solder Alloy Composition Effects

The most important effect of solder alloy composition on intermetallic formation is related to tin content of the solder. The high-tin content solders 95Sn-5Sb, 95Sn-5Ag, and pure tin all exhibit similar behavior with respect to intermetallic formation. In comparison to the pure tin, the 95Sn-5Sb solder exhibits a slightly lower parabolic rate constant for intermetallic formation with Cu-15Ni-8Sn. This could be associated with the antimony content of the η intermetallic layer, leading to a reduction in the interdiffusion rate of the compound. In contrast, the silver in the 95Sn-5Ag solder is rejected into the solder and tends to form the Ag_3Sn intermetallic layer distributed as discrete particles visible at the interface of the solder with the η intermetallic layer. These relatively small differences between the 95Sn-5Ag solder and 95Sn-5Sb solder with respect to intermetallic formation with Cu-15Ni-8Sn are not seen for pure copper or Cu-5Sn-0.2P. The relative intermetallic formation rates with Cu-9Ni-6Sn dependent on exposure temperature.

The high-lead content solders, 10Sn-90Pb, 5Sn-95Pb, and 10Sn-88Pb-2Ag form intermetallic compositions at a rate controlled by diffusion of tin through the solder. This is supported by the relative uniformity of intermetallic growth rates for 10Sn-90Pb in contact with a wide variety of base metals (Table 3), which have greatly different intermetallic growth rates when in contact with high-tin solders (*e.g.*, Fig. 5). An exception to this may be alloys with greater than 15% nickel at 250°C, for which diffusion through the intermetallic layer may be sufficiently slow in comparison to lower nickel content alloys as to be rate controlling. In addition, control of layer growth by diffusion through the solder is supported by the observation of a larger ratio of ϵ-Cu_3Sn to total layer thickness for pure copper and Cu-5Sn-0.2P soldered with 10Sn-90Pb, as compared to the same base metals with higher tin content solders. The growth of the η phase layer is limited by tin diffusion through the high-lead content solder, while the tin necessary for the growth of the ϵ phase is obtained by decomposition of Cu_6Sn_5 at the interface of the two intermetallic layers. Further, the slightly lower tin contents of 59 to 60 wt-% of the $(Cu,Ni)_6Sn_5$ formed on Cu-15Ni-8Sn soldered with 10Sn-90Pb, as compared to 60 to 62 wt-% for the η phase formed with higher tin content solders (Table 5), also suggests that tin diffusion through

the solder is limiting the rate of intermetallic layer growth. The lower rate of intermetallic formation for the Cu-15Ni-5Sn alloy with 5Sn-95Pb solder as compared to 10Sn-90Pb is also consistent with transport of tin through the solder as the rate-controlling step. The reason for the lower rate of intermetallic formation for Cu-15Ni-8Sn in contact with 10Sn-88Pb-2Ag solder as compared to 10Sn-90Pb is not as obvious. However, it is likely that precipitation of the Ag_3Sn intermetallic compound, seen as fine particles dispersed in the solder following elevated temperature exposure, reduces the tin content of the lead matrix, resulting in a decreased rate of transport of tin through the solder.

The intermetallic formation rate for the near eutectic 60Sn-40Pb solder is frequently higher than that for solders containing 10% or less tin or 95% or more tin. This is clearly seen in Fig. 8 for Cu-15Ni-8Sn alloy and can also be observed for Cu-5Sn-0.2P and Cu-9Ni-6Sn by comparison of Figs. 5-7. In the cases of pure copper or Cu-1.9Be-0.4Co in contact with 60Sn-40Pb, the parabolic rate constants are only slightly higher as compared to those for 95Sn-5Sb or 95Sn-5Ag. The increase in intermetallic formation rates with decreased tin content is rather difficult to account for. Results of other investigators (Ref. 6) show a maximum in intermetallic formation rate at the 60Sn-40Pb composition for tin-lead coatings electrodeposited on pure copper and heated at 170°C. The same authors show that a 5-micron-thick layer of electroplated lead between the copper and electroplated tin results in a 50% increase in the rate of intermetallic layer growth (Ref. 20). The increase in intermetallic formation rate in the presence of lead might be ascribed to an increased rate of transport of tin across the interface between the solder and the intermetallic formed. However, the parabolic kinetics of layer growth for the lead-free solders does not support the conjecture that intermetallic formation is surface reaction limited. Another possibility is that lead alloys with the intermetallic compound and this increases the diffusion rates of copper and tin in the intermetallic layer. If so, the lead content of the intermetallic composition must be quite low, since no lead could be detected by energy dispersive x-ray analysis.

Effects of Exposure Temperature

The effects of exposure temperature on intermetallic formation have been discussed in relation to base metal and solder alloy composition in the preceding sections. It is possible to compare the results obtained for pure copper to those obtained by other investigators in terms of the activation energies. The activation energy for intermetallic layer growth (total thickness) of 8800 to 12,600 cal/mol for pure copper and Cu-5Sn-0.2P soldered with 95Sn-5Sb measured in this investigation are somewhat higher than a value of 5800 cal/mol obtained for electrodeposited tin on pure copper, but lower than the activation energies in the range of 14,000 to 19,000 cal/mol obtained for interdiffusion of copper and tin in the ϵ and η phases (Ref. 21). The activation energies for intermetallic layer growth for copper and Cu-5Sn-0.2P in contact with 60Sn-40Pb solder of 14,000 to 16,000 cal/mol are higher than the value of 9300 cal/mol obtained for electrodeposited 60Sn-40Pb alloy over the temperature range 70° to 170°C. These differences are not surprising in view of the different nature of these experiments. The electrodeposits are considerably thinner than the solder layers used in this study and also show high initial growth rates over about the first 20 h which are not found here.

Conclusions

1. Copper and copper alloys react with tin-containing solders at elevated temperature to produce intermetallic compounds. The growth of the intermetallic layer follows parabolic kinetics and depends on the base metal composition, solder composition, and exposure temperature.

2. The rate of intermetallic formation between solders with 30% or more tin and copper-base alloys containing 0 to 30% nickel exhibits a distinct peak at nickel contents of 6 to 9%. Intermetallic formation rates may vary by a factor of 35, depending on nickel content. At 150°C (302°F), the rate is lowest for alloys containing 15% nickel or more. At 200°C (392°F), the rate is lowest for nickel-free alloys.

3. Distinct nickel-rich and nickel-poor layers of $(Cu,Ni)_6Sn_5$ form at temperatures of 175°C (347°F) and below on nickel-containing, copper-base alloys in contact with tin-containing solders. This effect is prominent in alloys containing 15% nickel or more and is associated with low rates of intermetallic layer growth for these alloys.

4. The rate of intermetallic formation between copper-base alloys and high-lead content solder (10% tin or less) at 200°C is much less than that for the high-tin content solders in this study. The rate of intermetallic formation between high-lead content solders and these copper-base alloys is relatively insensitive to base metal composition at 225°C (437°F) or below.

5. For all the copper alloys in this investigation, contact with 60Sn-40Pb solder at 175°C produces a greater intermetallic formation rate than does contact with solders containing 95% tin or more.

6. Selection of solders for copper-base alloys for applications at temperatures of 150°C and above requires that intermetallic formation be carefully considered. Lead-base solders with 10% tin or less may be required to control intermetallic formation during extended service at elevated temperatures.

Acknowledgments

The author would like to thank C. R. Scorey for useful discussions of this work, D. Beckwith for his contributions to the experimental work, L. Murray and G. Tomaino for SEM and x-ray diffraction analyses, and P. Novak for typing of the manuscript.

References

1. Lubyova, Z., Fellner, P., and Matiasovsky, K. 1975. Diffusion in the systems iron-tin and copper-tin. *Z. Metalldke* 66(3):179-182.

2. Saperstein, Z. P., and Howes, M. H. 1968. The reaction of α brass with lead-tin solders. *Welding Journal* 33(4):162-s to 172-s.

3. Tsuda, N., Tanabe, A., and Hirawata, K. 1978. The reaction of copper with Sn-Pb solder. *J. Jpn. Inst. Metals* 12(1):1-11.

4. Zakraysek, L. 1972. Intermetallic growth in tin-rich solders. *Welding Journal* 37(11):536-s to 541-s.

5. Kay, P. J., and MacKay, C. A. 1976. The growth of intermetallic compounds on common basis materials coated with tin and tin-lead alloys. *Trans. Inst. of Metal Finishing* 54: 68-74.

6. Schmitt-Thomas, K., and Hammer, M. 1977. Formation of intermetallic phases in soldered joints and the significance of these phases for the fracture behavior. *Schweissen und Schneiden* 29(7):258-262.

7. Gerth, D. 1970. Investigation of composition of diffusion layers in soft-soldered copper. *Metall.* 24(8):838-846.

8. Warwick, M. E., and Muckett, S. J. 1983. Observations on the growth and impact of intermetallic compounds on tin-coated substrates. *Circuit World* 9(4):5-11.

9. Davis, P. E., Warwick, M. E., and Muckett, S. J. 1983. Intermetallic compound growth and solderability of reflowed tin and tin-lead coatings. *Plating and Surface Finishing* 70:49-53.

10. Davis, P. E., Warwick, M. E., and Kay, P. J. 1982. Intermetallic compound growth and solderability. *Plating and Surface Finishing* 69: 72-76.

11. Audelo, A. 1973. Failure mechanism of tin plating in the solder industry. *Welding Journal* 38(10):454-s to 459-s.

12. Zakraysek, L. 1971. The effect of temperature and stress on tin-rich solder alloys. *Welding Journal* 36(12):522-s to 527-s.

13. Stone, K. R., Duckett, R., Muckett, S., and Warwick, M. E. 1983. Mechanical properties of solders and soldered joints. *Brazing and Soldering* (4):20-27.

14. Marinis, T. F., and Reinert, R. C. 1985. Isothermal aging characteristics of external lead solder connections. *Proc. 34th Electronic Components Conference,* pp. 73-80, I.E.E.E.

15. Saperstein, Z. P., and Howes, M. H.

1969. Mechanical properties of soldered joints in copper alloys. *Welding Journal* 34(8):317-s to 327-s.

16. Scorey, C. R., and Ward, W. T. 1983. Pfinodal C72900: A new spinodal copper alloy for burn-in test sockets. *Sixteenth Annual Connectors and Interconnection Technology Symposium Proceedings:* 141-148. Electronic Connector Study Group.

17. Scorey, C. R., Chin, S., White, M. J., and Livak, R. J. 1984. Spinodal Cu-Ni-Sn alloys for electronic applications. *Journal of Metals* 36 (11):52-54.

18. Fister, J. C., and Breedis, J. F. 1983. Copper alloys for avoidance of interdiffusion in electronic packages. Unpublished abstract presented at *The 3rd Annual Electronics Packaging Conference.*

19. Bakker, H., *et al.* 1985. Defects, disordering and mobility in intermetallic compounds. *Diffusion in Solids: Recent Developments.* eds. M. A. Dayanada and G. E. Murch. pp. 39-65, The Metallurgical Society.

20. Kay, P. J., and MacKay, C. A. 1979. Barrier layers against diffusion. *Trans. Inst. of Metal Finishing* 57:169-174.

21. Butrymowicz, D. B. 1981. *Diffusion Rate Data and Mass Transport Phenomena for Copper Systems.* p. 428, International Copper Research Assoc.

Appendix

Statistical Analysis of Parabolic Rate Constants

This appendix describes the methods used to analyze the intermetallic layer thickness measurements in order to obtain a best estimate of the parabolic rate constant and to quantify the uncertainty associated with that estimate. Due to the large numbers of specimens in this study arising from the combinations of the base metal, solder composition, exposure temperature and exposure time, it is not practical to compensate for the variability in thickness measurements by computing the mean of a very large number of thickness measurements performed on each specimen. In general, the number of thickness measurements were limited to five for each specimen condition at the expense of some loss in precision in determining the rate of intermetallic layer formation. In order to both minimize and quantify the uncertainty in intermetallic layer formation rate associated with both the limited number of thickness measurements made and the limited number of exposure times evaluated, the following analysis of the intermetallic measurements has been used:

It is assumed that the intermetallic formation can be described by diffusion-controlled layer growth with parabolic kinetics

$$x = kt^{1/2} \tag{1}$$

in which x is the thickness of the intermetallic layer (or layers), t is exposure time, and k is the parabolic rate constant. Examination of the soldered specimens prior to exposure indicated a negligible quantity of intermetallic layers (less than 1 micron) formed during soldering, with the exception of Cu-1.9Be-0.4Co soldered with high-tin solders, which results in a 3- to 6-micron-thick layer of intermetallic compound as-soldered. In these cases, it is assumed that the kinetics can be described as

$$(x^2 - x_0^2)^{1/2} = kt^{1/2} \tag{2}$$

in which x_0 is the mean initial intermetallic layer thickness formed during soldering. An analysis of measurements on 120 individual specimens indicates that the standard deviation in the thickness measurement σ_x can be expressed as a function of the mean thickness x by

$$\sigma_x = bx^m \tag{3}$$

in which the exponent m has a value of 0.75 and the constant b has a value of 0.4 microns. (The value of m lies between a value of m = 1 for a log normal distribution and m = 0 for a normal distribution.) This effect can be seen qualitatively in Fig. 2 as an increase in the standard deviation in intermetallic thickness measurements with increased mean layer thickness.

In order to determine the parabolic rate constant for a normal distribution, Equation 1 was transformed to

$$x' = k'(t')^{0.5} \tag{4}$$

in which

$$x' = x^{0.25}$$
$$t' = t^{0.25}$$
$$k' = k^{0.25}$$

The value of k′ is determined as that which minimizes the standard error in x′, expressed as

$$(S_{x'})^2 = \sum_{L=1}^{n} \left[\frac{x'_L - k'(t'_L)^{0.5}}{n} \right]^2 \tag{5}$$

in which n is equivalent to the number of specimens examined. An estimate of the uncertainty in k′ is obtained as plus or minus $2S_x'$ limits. The values of $k = xt^{-0.5}$ associated with these limits for a total of n measurements are $[k' + 2S_x/(t'n)^{0.5}]^4$ and $[k' - 2S_x/(t'n)^{0.5}]^4$. These limits for the parabolic rate constant using a value of t′ equivalent to the longest exposure period are shown as error bars in Figs. 3, 5 and 6, and are listed as uncertainty limits in Table 3.

This procedure for calculating parabolic rate constants, while somewhat more complicated than a simple linear regression analysis, does not unduly bias the calculated rate constant, due to a single, long-time measurement which has significant variation associated with it. The characterization of intermetallic layer growth by a single parabolic rate constant facilitates the description of the effect of alloy composition, solder composition, and exposure temperature on intermetallic formation behavior.

Reminder to Authors

Please note that completed Author Application Forms and accompanying 500- to 1000-word summaries must be mailed by July 15, 1987, to ensure consideration for the Professional Program of the 69th Annual AWS Convention, to be held April 17–22, 1988, in New Orleans, La. Author Application Forms appear opposite page 128-s in the April 1987 issue of the *Welding Journal.*